Frequency Regulation at a Wind Farm Using Time-Varying Inertia and Droop Controls

Yuan-Kang Wu, Wu-Han Yang, Yi-Liang Hu, and Dung Phan Quoc

Abstract -- **As renewable power generation becomes more prevalent, the problem of frequency stability has become a particular concern of transmission system operators (TSOs), especially those of small power transmission systems. Traditional wind generation systems do not provide frequency regulation because they are decoupled from the power grid. Therefore, as conventional thermal generators are replaced by wind generators, the issue of frequency regulation for wind generation systems has become increasingly important. To release the kinetic energy stored in the rotating mass, inertia and droop control loops can be added into the controller of a wind turbine (WT). This work proposes an advanced control strategy with the time-varying gains of two control loops. In the proposed strategy, the gains are determined based on the desired frequency-response time. Moreover, the initial gain of the control loop is determined based on the wind speed, considering the operating condition of each WT in a wind farm (WF). The effectiveness of the proposed method is verified using an actual power system, revealing that it can be used to improve frequency regulation in a power grid.**

Index Terms— **Frequency stability, Wind generation, Inertia and droop control loops, Power System, Frequency regulation.**

NOMENCLATURE

J	Moment of inertia
ω_m	Angular frequency of a machine
T_m	Mechanical torque
T_{em}	Electromagnetic torque
P_m	Mechanical power
P_{em}	Electromagnetic power
H	Inertia constant
ω_s	Synchronous angular frequency of a machine
S_{mach}	Rated apparent power of a machine
$\overline{\omega_m}$	Angular frequency of a machine in per unit
$\overline{P_m}$	Mechanical power in per unit
$\overline{P_{em}}$	Electromagnetic power in per unit
K	Inertia response constant
$\Delta\overline{P_r}$	Variance of power on the rotor kinetic energy in per unit
$\Delta\overline{E_{k,r}}$	Variance of energy on the rotor kinetic energy in per unit
$\overline{\omega_{mo}}$	Initial angular frequency on the rotor kinetic energy in per unit
$\Delta\overline{P_g}$	Variance of power in per unit
$\Delta\overline{E_{k,g}}$	Variance of energy in per unit
$\overline{\omega_s}$	Synchronous angular frequency of a machine in per unit
$\overline{\omega_{so}}$	Initial synchronous angular frequency in per unit
$\overline{\omega_i}$	Angular frequency of a machine in per unit at V_i
$\overline{\omega_{\min}}$	Minimum angular frequency of a machine in per unit
$\overline{\omega_{\max}}$	Maximum angular frequency of a machine in per unit
$-\dfrac{1}{R_o}$	Slope of droop control
$\Omega_{m\_\min}$	Minimum mechanical speed
$\Omega_{m\_\max}$	Maximum mechanical speed
V_{in}	Cut-in wind speed
$V_{\Omega_{m\_\min}}$	MPPT start-up wind speed
$V_{\Omega_{m\_\max}}$	MPPT cut-off wind speed
V_{nom}	Nominal wind speed
V_{out}	Cut-out wind speed
f_{nom}	Nominal frequency
$f_{measured}$	Measured frequency
$f_{\min}$	Minimum allowable frequency
$f_{\max}$	Maximum allowable frequency

I. INTRODUCTION

As awareness of the importance of environmental protection increases, more countries are becoming interesting in the development of renewable sources. Wind energy is the most abundant renewable source of energy in western Taiwan. The government has legislated for the integration of a large amount of wind energy into Taiwan's power system. Frequency stability is important to ensuring that the power system can withstand the intermittent disturbances from renewable generation. Two types of wind turbines are commercially popular. The first, Type 3, is the doubly fed induction generator (DFIG); the other, Type 4, is the full-rated converter wind generator. However, their frequency dynamic responses are decoupled from the power grid. As the penetration of variable-speed wind turbine generator into a

power systems increases, frequency variations become larger whenever a contingency arises in power system, and especially in an isolated power grid. Therefore, the frequency regulation of wind turbines is becoming increasingly important. This work proposes a new frequency regulation strategy and improves the frequency dynamic characteristics of an island power system. The demonstration of this strategy provides a reference for power system operators and wind farm managers.

The variable-speed wind turbines that are commercially and predominantly used nowadays have no inherent inertia response or primary frequency response. As traditional thermal units are gradually replaced by wind generators, wind turbines are likely to include frequency regulation to support the power system. Inertia responses [1-3] and speed droop response [4] limit the rate of change of frequency (ROCOF) and improve the frequency nadir (FN) during an imbalance between generation and load. Combining the inertia with droop responses is an alternative method for improving FN [5-8]. Since the kinetic energy that is stored in the rotational mass is mechanically decoupled from the power grid and does not automatically contribute an inertia response to the power system, double-fed induction generators cannot improve frequency stability. However, Type 3 and Type 4 wind generators can be made to provide inertia and droop responses using appropriate control loops. Many investigations have discussed this topic and constructed various models to provide frequency regulation. As penetration by wind power increases, wind turbines with beneficial inertia and droop responses will become increasingly necessary.

Many researches have discussed the frequency regulation capability of a DFIG-based WT. References [1, 9] presented the simple and fundamental concept of inertia control and compared the responses of fixed-speed induction generators and DFIGs. Reference [4] discussed the mathematical formulation of the inertia response of wind turbines. References [10-11] optimized the integration of inertia control and droop control into a wind turbine using inertia response, rotor speed control and pitch angle control, to implement coordinate control. To protect the wind turbine from stalling, the appropriate parameters of the inertial and droop controllers must be selected [11].

D. Margaris et.al. investigated the Rhode Island power grid, which is an autonomous system [7]. They studied transient frequency support (inertia response), permanent frequency regulation (droop control) and the integrated application of these concepts. These characteristics were quantitatively analyzed to elucidate the expected benefits and drawbacks of each method, yielding a suggested 10% reserve to ensure favorable capacity, considering both effective adjustment of reserve and the minimization of energy loss. To increase the efficiency and benefit of the frequency regulation, reference [12] used a super-capacitor that was connected to the DC-link of a back-to-back inverter. Reference [13] continuously adjusted the droop value of the wind turbine in response to wind velocity. Reference [14] presented a novel

strategy that was based on the use of the kinetic energy of rotating masses to reduce the need for the de-loading operation while providing the required power reserve. Reference [15] conducted a small-signal analysis to examine the frequency response of power systems. Reference [16] utilized a novel probabilistic method to estimate the aggregate inertia response, in which wind turbulence was modeled using a Gaussian probability distribution.

Each WT in a wind farm contains different levels of releasable kinetic energy because of the wake effect [17-19]. Therefore, compared to the constant gain control scheme, a control scheme with stable and adaptive gain was proposed in [17, 18]. The values of two loop gains are proportional to the kinetic energy stored in a DFIG-based WT to utilize the releasable kinetic energy. In [19], the impact of wake effect on the WT inertia response is analyzed. The simulation is compared with the measured data.

The electrical frequency of a power grid must be maintained very close to its nominal frequency; otherwise excessive frequency excursion may cause load shedding, instability or even blackout. The declining inertia and primary frequency response, arising from inverter-coupled generation, are increasing concerns in the power industry. References [20-21] considered wind power penetration scenarios for the U.S. Western Interconnection and U.S. Eastern Interconnection, respectively, to assess the effect of various active power control strategies on the frequency response. Although the inertia response that is provided by wind turbines has been discussed by the industry, only a very few of today's grid codes include relevant specific requirements. Reference [22] summarized and assessed two years of operations of the Canadian province, Quebec, focusing on inertia response.

In the traditional control scheme, the inertia and droop gains are constants. This work proposes a new control methodology concerning the frequency regulation using time-varying K and R values in the control loops. The inertia and droop control algorithms are established according to the fundamentally mathematical equations. Additionally, a DFIG-based WT model that combines inertia control, rotor speed control and pitch angle control is used for simulations. Different levels of wind power penetration are considered herein to validate the flexibility and efficiency of the proposed method.

This work is organized into five sections. Section II introduces the fundamental concept of inertia control and proposes a new inertia control method. Section III presents the fundamental concept of droop control and develops a new droop control algorithm. Section IV demonstrates the results of a simulation of the new control method and an island power system with various wind velocities and degrees of penetration. Finally, Section V draws conclusions and lists the contributions of this work.

II. INERTIA CONTROL STRATEGY

A. Fundamental Concept of Inertia Control

Since it is decoupled from the power grid, a wind turbine generator cannot exhibit inertia and droop responses when a contingency arises in the power system. Figure 1 shows a general frequency regulation model for a wind turbine generator. $\Delta P_{inertia}$ denotes the inertia response (solid red line) and ΔP_{droop} represents the droop response (dashed blue line). While a variation between the measured and the nominal frequency is detected, the corresponding responses are determined by their individual functions. Multiplying the swing equation, Eq. (1), by ω_m yields the power balance equation, Eq. (2).

$$J\frac{d\omega_m}{dt} = T_m - T_{em} \tag{1}$$

$$J\omega_m\frac{d\omega_m}{dt} = P_m - P_{em} \tag{2}$$

The inertia constant H is expressed by Eq. (3) and defined as the ratio of the stored kinetic energy at synchronous speed to the machine rating. Then, the power balance equation in per-unit can be derived as Eq. (4).

$$H = \frac{\frac{1}{2}J\omega_s^2}{S_{mach}} \text{ MJ/MVA} \tag{3}$$

$$2H\overline{\omega_m}\frac{d\overline{\omega_m}}{dt} = \overline{P_m} - \overline{P_{em}} \tag{4}$$

The fundamental concept of the inertia response is that the appropriate K value in Eq. (5) can be obtained by comparing this equation with Eq. (4), to efficiently determine the inertia response and to prevent DFIGs from stalling.

$$K\overline{\omega_m}\frac{d\overline{\omega_m}}{dt} = \overline{P_m} - \overline{P_{em}} \tag{5}$$
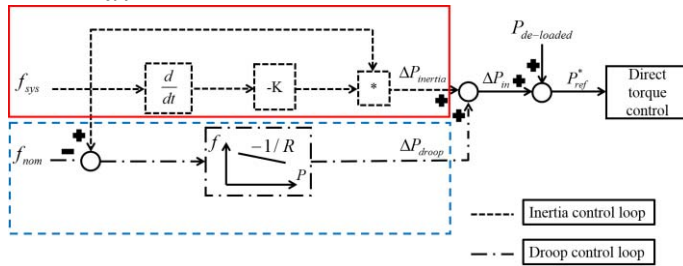

Fig. 1. Frequency regulation of wind turbine generator [11].

B. Proposed Inertia Control Strategy

Each wind turbine generator in a wind farm receives wind at a different velocity as a result of the wake effect. Accordingly, different K values should be used to maximize the inertia response. Therefore, finding these values and ensuring that the DFIG does not stall is important. In this work, the principle of conservation of energy is applied to the rotor kinetic energy to develop a new inertia control strategy.

From the various wind velocities, one can calculate potential maximum initial K values, and ultimately converge to the minimum K value in a particular period. Accordingly, the wind turbine can provide more inertia in the initial period when a fault occurs and reduce the oscillation of frequency in the period of convergence.

The power balance function of the rotor kinetic energy is obtained from Eq. (6). The rotor kinetic energy function is obtained by integrating Eq. (6) to yield Eq. (7).

$$\Delta\overline{P_r} = 2H\overline{\omega_m}\frac{d\overline{\omega_m}}{dt} = \overline{P_m} - \overline{P_{em}} \tag{6}$$

$$\Delta\overline{E_{k,r}} = \int\Delta\overline{P_r}dt = \int 2H\overline{\omega_m}\frac{d\overline{\omega_m}}{dt}dt = H\int d\overline{\omega_m}^2 = H(\overline{\omega_m}^2 - \overline{\omega_{mo}}^2) \tag{7}$$

The power balance function of power grid energy is given by Eq. (8), which is integrated to yield Eq. (9), which is the power grid energy function.

$$\Delta\overline{P_g} = K\overline{\omega_s}\frac{d\overline{\omega_s}}{dt} \tag{8}$$

$$\Delta\overline{E_{k,g}} = \int\Delta\overline{P_g}dt = \int K\overline{\omega_s}\frac{d\overline{\omega_s}}{dt}dt = \frac{K}{2}\int d\overline{\omega_s}^2 = \frac{K}{2}(\overline{\omega_s}^2 - \overline{\omega_{so}}^2) \tag{9}$$

The principle of conservation of energy, applied to the rotor kinetic energy and the power grid energy, requires that Eq. (7) equals Eq. (9), from which Eq. (10) is derived for the value of K.

$$K = 2H\frac{\overline{\omega_m}^2 - \overline{\omega_{mo}}^2}{\overline{\omega_s}^2 - \overline{\omega_{so}}^2} \tag{10}$$

According to reference [11], when a contingency arises in a DFIG, the rotor speed can be increased the range from 0.6 p.u. to 1.3 p.u.. This work assumes that the nominal frequency is 50 Hz, the load shedding frequency is 48, and the maximum allowed frequency is 52 Hz. Percentage frequency variations in the range $\pm 4\%$ are tolerated. Based on the work of reference [11], which considered the worst-case situation, the general values of K that can be used at all wind velocities when the system frequency varies. $K_{general\_rise}$, given by Eq. (11), is defined as the general value when the system frequency rises, and $K_{general\_drop}$, given by Eq. (12), is the general value as the system frequency falls. To minimize the oscillation of frequency in the period of convergence, K_{final}, which is directly proportional to $H(\overline{\omega_m}^2 - \overline{\omega_{mo}}^2)$, is defined, based on the work of reference [17]. Finally, K_{final} values at a particular wind velocity as the system frequency is rising and falling are derived as Eqs. (13) and (14), respectively.

$$K_{general\_rise} = 2H\frac{1.3^2 - 1.2^2}{1.04^2 - 1^2} = 6.1275H \tag{11}$$

$$K_{general\_drop} = 2H\frac{0.6^2 - 0.7^2}{0.96^2 - 1^2} = 3.3163H \tag{12}$$

$$K_{final} = K_{general\_rise} \frac{(\overline{\omega}_{max}^2 - \overline{\omega}_i^2)}{(\overline{\omega}_{max}^2 - \overline{\omega}_{min}^2)} \qquad (13)$$

$$K_{final} = K_{general\_drop} \frac{(\overline{\omega}_{min}^2 - \overline{\omega}_i^2)}{(\overline{\omega}_{min}^2 - \overline{\omega}_{max}^2)} \qquad (14)$$

K_{final} is the final value of inertia during a grid fault at a particular wind velocity. To enable the inertia response at different wind speeds to be used, accounting for the wake effect, $K_{initial}$, which represents the kinetic energy that is initially stored in the rotor mass, is defined as in Eq. (15).

The new inertia response is obtained by using $K_{initial}$ and K_{final} to generate a mathematical function for the inertia response during the grid fault, in which the initial inertia response is maximal and the oscillation of frequency is minimal at a given wind velocity.

$$K_{initial} = 2H \frac{\overline{\omega}_m^2 - \overline{\omega}_i^2}{\overline{\omega}_s^2 - \overline{\omega}_{so}^2}, \quad \overline{\omega}_m = \begin{cases} \overline{\omega}_{max} & , \ f_{measured} > f_{nom} \\ \overline{\omega}_{min} & , \ f_{measured} < f_{nom} \end{cases} \qquad (15)$$

The function of time-varying inertial gain is illustrated in Fig. 2. Before the frequency drops, the inertial gain is on the initial value $K_{initial}$ determined by Eq. (15). As the frequency drops, the K reduces. Finally, the inertial gain reaches K_{final}, determined by (14). The desired response time when the inertial gain varies from $K_{initial}$ to K_{final} is denoted by $\Delta t_{desired}$. According to different design requirements, various time-varying functions can be selected. This work selects the parabolic function, as shown in Fig. 2, because the parabolic function maintains a large K in the beginning of the fault.
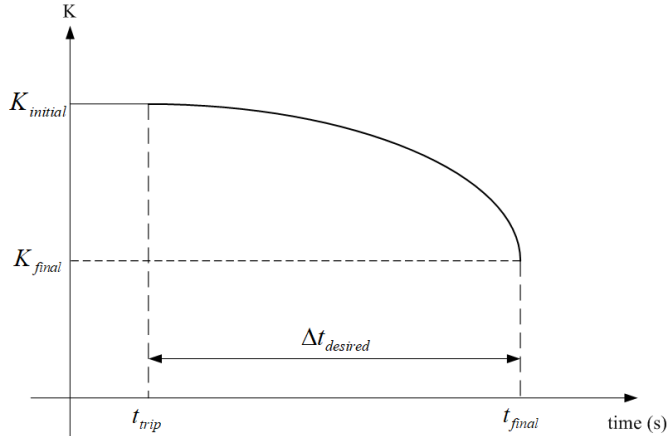

Fig. 2. Time-varying inertial gain described by the parabolic function during the frequency drop

III. DROOP CONTROL STRATEGY

A. Fundamental Concept of Droop Control

A wind turbine can use its rotor speed control or pitch angle control to implementation its de-loading operation model to enable sufficient power reserve to be available to eliminate the frequency excursion when a contingency arises in the power system. To provide frequency regulation of the wind turbine, such characteristics of a traditional synchronous generator such as speed droop control must be used. Many studies have discussed the issue of de-loading control but not accurately or mathematically quantified the inertial K and droop R values. In this section, the rotor speed and pitch angle are obtained using Matlab software and their values are input to PSCAD/EMTDC power system software.

Figure 3 displays the characteristic of droop control, as defined in this work. This concept is very similar to that associated with a conventional synchronous generator. Before a contingency occurs, the wind turbine is operated at point $P_{de-loaded}$ to have sufficient power reserve to support any frequency excursion. However, when a contingency arises in the power system, the reachable maximum power may increase to P_{MPPT}. ΔP is determined by the variation between the nominal frequency and the measured frequency. According to reference [7], when both the economic benefit and frequency regulation are considered, 90% de-loading is the best selection compared to 80% or 70% de-loading operations. Figures 4 plots the power curve for the de-loading operations and the right curve beside the MPPT curve, rather than the left curve, is used in this de-loading control because doing so causes the wind turbine to operate stably state, as explained by reference [12]. Inertia control supports a rapid transient response but droop control provides slow permanent regulation of the power system.
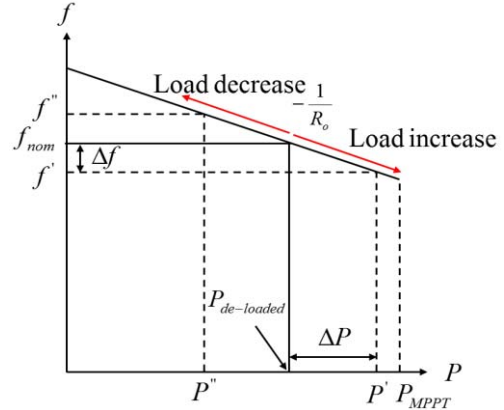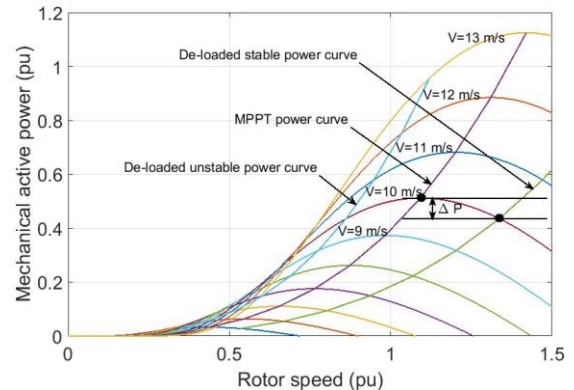

Fig. 3. Droop control of a wind turbine generator.

Fig. 4. De-loading power curve.

B. Proposed Droop Control Strategy

To support optimally the active power from a wind turbine during grid disturbances, it is required to calculate the optimal rotor speed and the pitch angle values at various wind velocities. Figure 5 presents the operating principle concerning the rotor speed regions, and the pitch angle is determined by the power-coefficient function. The solid black curve corresponds to a wind turbine that is operated according to the MPPT mode and the dashed red curve corresponds to one operated according to the de-loading mode. The slope of the curve in region $2_{(new)}$ is larger than that in region 2. Thus, as the wind speed increases, the rotor speed of de-loaded model increases greatly. In addition, because the wind speeds of region $2_{(new)}$ are smaller than those of region 2, the de-loaded curve shifts to the left.

The de-loaded model also consists of four operating regions. If the wind speed is between V_{in} and $V_{\Omega_{m\_min}}(new)$, the operation lies in region $1_{(new)}$. When the wind speed exceeds $V_{\Omega_{m\_min}}(new)$, the operation model enters into region $2_{(new)}$, in which the rotor-speed control is utilized to achieve the desired power reserve. However, if the wind speed is lower than $V_{\Omega_{m\_min}}(old)$, the power reserve is less than the desired value.

The operation model enters into the region $3_{(new)}$ when the wind speed exceeds $V_{\Omega_{m\_max}}(new)$. This region consists of two parts. When the wind speed is lower than $V_{\Omega_{m\_max}}(old)$, the desired power reserve cannot be achieved by the rotor-speed control only. Thus, both rotor-speed control and pitch-angle control should be applied simultaneously. However, the rotor-speed control and the pitch-angle control are electrical and mechanical operations, respectively. From the viewpoint of response time, the speed of rotor-speed control is fast. Therefore, the rotor-speed control should be applied prior to the pitch-angle control.

As the wind speed exceeds $V_{\Omega_{m\_max}}(old)$, only the pitch-angle control is applied. As the rotor speed is at its maximum, there is no capability to store reserve power via the rotor-speed control. Consequently, the only method is to utilize pitch-angle control to store reserve power at a partial load operation. In region 4, the pitch-angle control is applied to store reserve power at a full load operation. Comparing to a normal operation with de-loaded model, the pitch angle of de-loaded model is greater than that during the normal operation in the same wind speed.

To optimize the R_o value of a wind turbine during a contingency, Matlab software is used to calculate the extreme slope of R value at various wind velocities under the de-loading operating mode. The required R_o value is set as determined by the frequency variation at each wind speed, guaranteeing the stable operation of the DFIG. Equations (16)

and (17) define R_o during the rising and falling of the frequency of the power system, respectively.

$$R_o = -\frac{f_{max} - f_{nom}}{P_{MPPT} - P_{de-loaded}} \times \frac{f_{max} - f_{nom}}{f_{measured} - f_{nom}}, for\, f_{measured} > f_{nom} \quad (16)$$

$$R_o = -\frac{f_{min} - f_{nom}}{P_{de-loaded} - P_{MPPT}} \times \frac{f_{min} - f_{nom}}{f_{measured} - f_{nom}}, for\, f_{measured} < f_{nom} \quad (17)$$
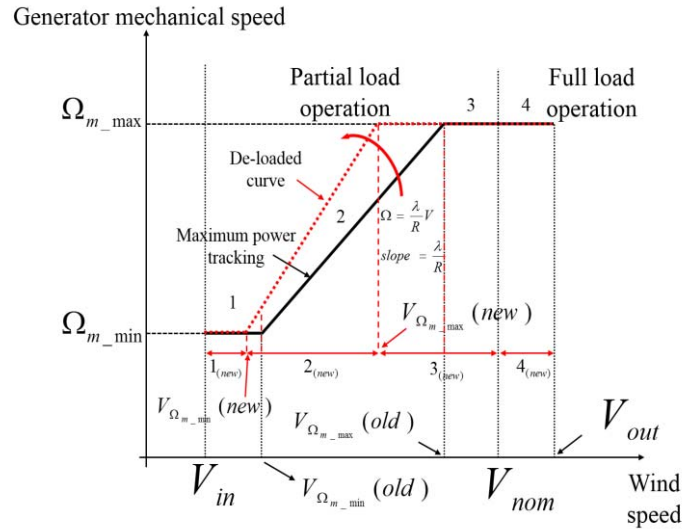

Fig. 5. De-loading rotor speed regions of DFIG.

IV. SIMULATION OF AN ISLAND POWER SYSTEM

To verify the feasibility of the proposed coordinate control, various scenarios associated with an island power system are compared. Figure 6 presents a single line diagram of an island power system. The highest voltage level is 69 kV and the system has 12 traditional generators and two 69 kV transmission lines. Load demand is approximately in the range of 35 MW to 81.5 MW.

The performances of different control strategies are compared under two different load demands. Coordinate control strategy is implemented and compared to no control, inertial control and droop control situations. The light load demand 35 MW and heavy load demand 81.5 MW are chosen as two extreme scenarios. In the simulation, the wind speed is 10 m/s. When the droop and coordinate controls are applied, the power reserve for each wind turbine is 10%. The overall installed wind power generation capacity is approximately 12.4 MW and the load demand is actual measured data. The simulations are as follows.

In this work, the frequency-response simulations are implemented by an N-1 contingency, in which a traditional thermal power generator trips offline. During the system contingency, the transient frequency response, the power output from the wind farm, and the rotor speed of a WT are recorded. To confirm the effectiveness of the proposed control method, the inertia gain K and the droop gain R during the fault are also observed.
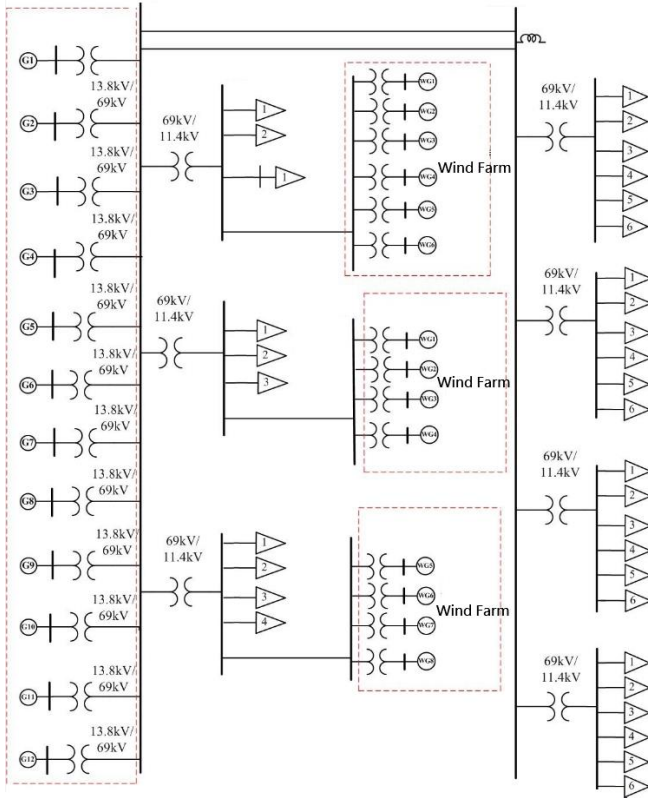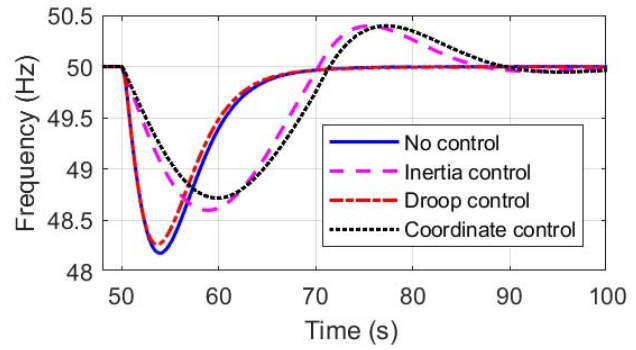
Fig. 6. Single line diagram of an island power system.
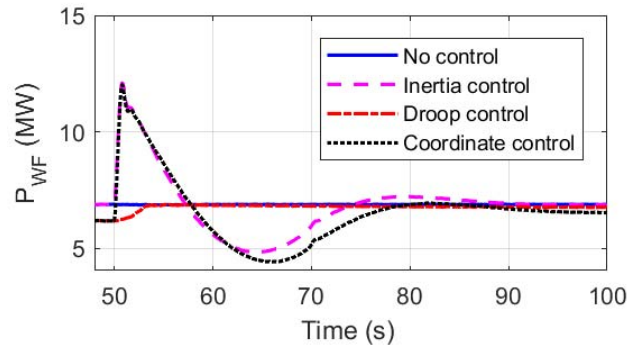
A. Light Load Demand 35MW

The simulation results in the scenario of light load demand are shown in Figs. 7 and 8. The frequency nadir in Fig. 7(a) is 48.53 Hz, 48.84 Hz, 48.58Hz, and 48.90 Hz, respectively, with no control, inertia control, droop control, and coordinate control strategy. Obviousely, the coordinate control has the highest frequency nadir compared to other control strategies during an N-1 contingency; moreover, inertia control is better than droop control. The active power output of the WF is shown in Fig. 7(b). It reveals that the power output increases at the moment using the the inertia or the coordinate control. Therefore, the rotor speed reduces greatly to release the rotating energy, as shown in Fig. 7(c).

Figure 8 shows the time-varying inertia and droop gains in this scenario, in which the initial inertia gain of the inertia controller and the coordinate controller is 78.94 and 105.70, respectively. After 20s, the inertia gain of them is reduced to 20.00 and 26.77, respectively. The large K value represents high inertia support. As shown in Fig. 8(b), the bend point of R curve is approximate 3.77 and 6.28, respectively, using the droop control and the coordinaate control. Small R values can provide high droop response characteristics.
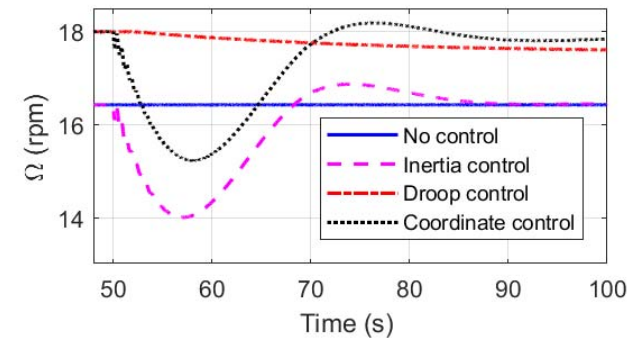
According to the above studies, the potential frequency regulation should include both inertia and droop controls to release rotating energy from a wind turbine. The simulation results reveal that the coordinate control strategy provides the best frequency response among various control methods during an N-1 contingency.
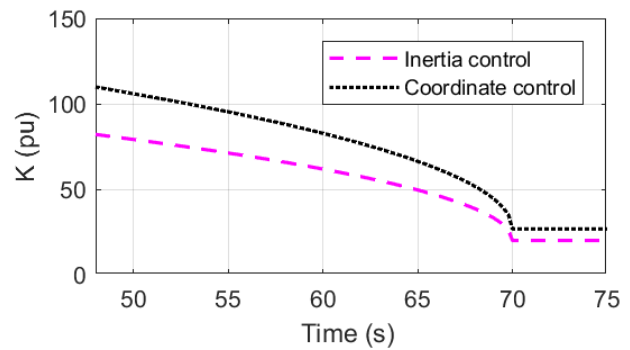

(a)

(b)

(c)

Fig. 7. Simulation results of light load demand 35 MW. (a) Frequency response, (b) The power output from the wind farm, (c) The rotor speed of a DFIG-based WT
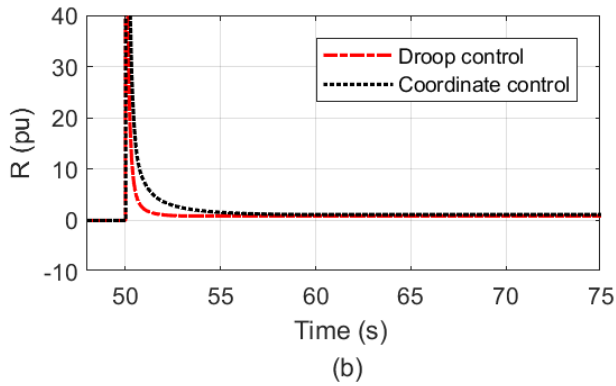

(a)

(b)

Fig. 8. Simulation results of light load demand 35 MW. (a) inertia gain (b) droop gain

B. Heavy Load Demand 81.5MW

The simulation results in the scenario of heavy load demand are shown in Figs. 9 and 10. As a contingency occurs, the frequency nadir drops to 48.61 Hz, 48.69 Hz, 48.63Hz, and 48.82 Hz, respectively, with no control, inertia control, droop control, and coordinate control strategy. The coordinate control has the highest frequency nadir compared to other control strategies during an N-1 contingency. However, the effect is not obvious compared to the operating scenario - light load demand.

The active power output of the wind farm is shown in Fig. 9(b). It indicates that the power output increases at the moment using the the inertia or the coordinate control. Therefore, the rotor speed reduces greatly to release the rotating energy, as shown in Fig. 9(c). Figure 10 shows the time-varying inertia and droop gains in this scenario. The K values are the same as those at light load demand because of the identical control mechanism.

As shown in Fig. 10(b), the bend point of R curve is approximate 4.09 and 6.62, respectively, using the droop control and the coordinaate control. The simulation results also reveal that the coordinate control strategy has the best frequency response among three different controls during an N-1 contingency.
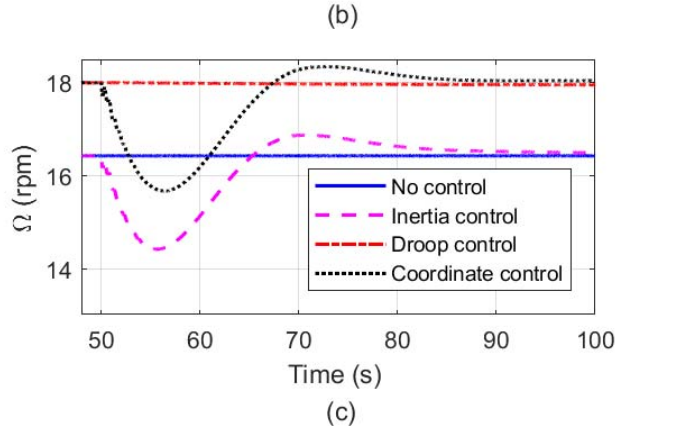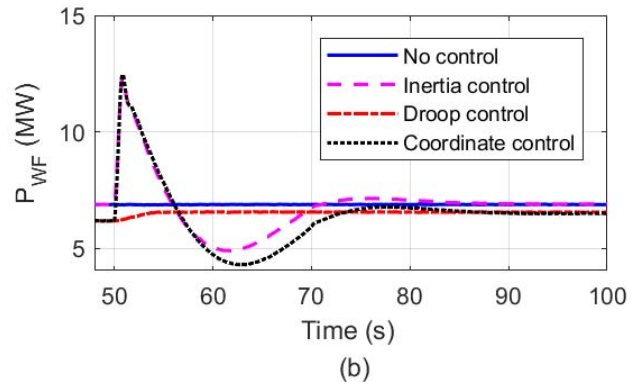

(b)

(c)

Fig. 9. Simulation results of heavy load demand 81.5 MW. (a) Frequency response, (b) The power output from the WT, (c) The rotor speed of a DFIG-based WT
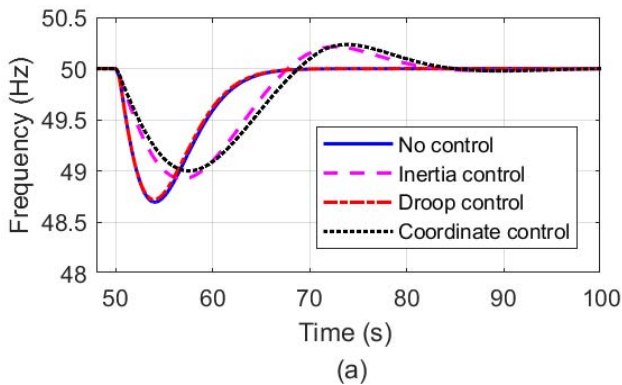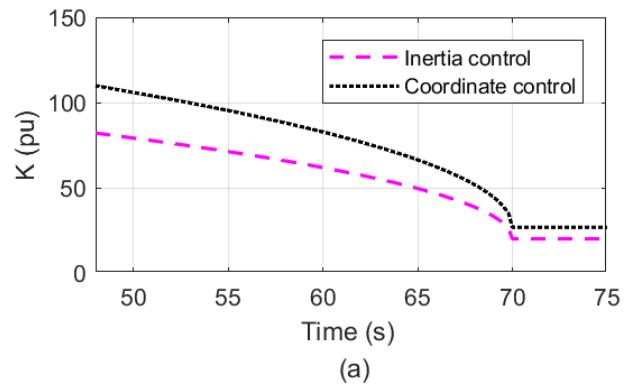

(a)

(a)

(b)

Fig. 10. Simulation results of light load demand 81.5 MW. (a) inertia gain (b) droop gain

The frequency nadirs using the four control schemes are summarized in Table I. The frequency nadirs without the frequency control are the lowest. Droop control cannot raise the frequency nadir greatly because the power reserve is only 10%. By contrast, the inertia and coordinate controls can raise the frequency nadir significantly because the wind farm can provide more active power support by releasing the rotating energy. The coordinate control provides the best freqnency response because the power increase from the wind farm is the largest.

TABLE I
FREQUENCY NADIRS USING THE FOUR CONTROL STRATEGIES

	Frequency nadir in the light load (Hz)	Frequency nadir in the heavy load (Hz)
Without Control	48.1800	48.6979
Inertia Control	48.5990	48.9254
Droop Control	48.2647	48.7215
Coordinate Control	48.7178	49.0021

ACKNOWLEDGMENT

V. CONCLUSIONS

As the wind power penetration increases and more traditional units are replaced by wind generators, maintaining power system stability becomes increasingly difficult. Therefore, many grid codes in several countries require that wind generators must exhibit frequency regulation to enhance the performance of the power grid into which they are connected. Frequency regulation usually involves the addition of a control loop in the RSC circuit. Unlike the traditional method for frequency regulation, the method that is developed herein involves the calculation of optimal K and R values; the proposed method is validated using an island power system. Furthermore, coordinate control that combines a parabolic function for the K variable and the 90% de-loading operating mode is implemented and its feasibility is verified. The main contributions of this paper are as follows.

1. Define the time-varying K value of the inertia loop and the time-varying R variable of the droop loop to prevent a DFIG from stalling and to obtain better inertia and droop controls.
2. Deduce the inertia and droop control algorithms from fundamental mathematical equations and establish a new coordinate control strategy for the frequency regulation of DFIGs.
3. Validate and establish the feasibility of the proposed coordinate control strategy with reference to an island power system with different load demands and penetration levels.

REFERENCES

[1] J. Ekanayake and N. Jenkins, "Comparison of the Response of Doubly Fed and Fixed-speed Induction Generator Wind Turbines to Changes in Network Frequency," *IEEE Transactions on Energy Conversion*, vol. 19, no. 4, pp. 800-802, 2004

[2] G. Lalor, A. Mullane and M. O'Malley, "Frequency control and wind turbine technologies," *IEEE Transactions on Power Systems*, vol. 20, no. 4, pp. 1905-1913, Dec. 2004

[3] M. Kayikci and J. V. Milanovic, "Dynamic contribution of DFIG-based wind plants to system frequency disturbances," *IEEE Transactions on Power Systems*, vol. 24, no. 2, pp. 859-867, May 2006.

[4] J. Morren, J. Pierik and S. W. H. D. Haan, "Inertia Response of Variable Speed Wind Turbines," *Electric Power Systems Research,* vol. 76, no. 11, pp. 980-987, 2006.

[5] J. Morren, S. Haan, W. L. Kling and J. A. Ferreira, "Wind turbines emulating inertia and supporting primary frequency control," *IEEE Transactions on Power Systems*, vol. 21, no. 1, pp. 433-434, Feb. 2006

[6] G. Ramtharan, J. B. Ekanayake and N. Jenkins, "Frequency support from doubly fed induction generator wind turbines," *IET Renewable Power Generation*, vol. 1, no. 1, pp. 3-9, Mar. 2007

[7] I. D. Margaris, S. A. Papathanassiou, N. D. Hatziargyriou, A. D. Hansen and P. Sorensen, "Frequency Control in Autonomous Power Systems with High Wind Power Penetration," *IEEE Transactions on Sustainable Energy*, vol. 3, no. 2, pp. 189-199, 2012

[8] J. F. Conroy and R. Watson, "Frequency response capability of full converter wind turbine generator in comparison to conventional generation," *IEEE Transactions on Power Systems*, vol. 23, no. 2, pp. 189-199, May 2008

[9] J. Ekanayake, L. Holdsworth and N. Jenkins, "Control of DFIG Wind Turbines," *Power Engineer*, vol. 17, no. 1, pp. 28-32, 2003

[10] H. T. Ma and B. H. Chowdhury, "Working Towards Frequency Regulation with Wind Plants: Combined Control Approaches," *IET Renewable Power Generation*, vol. 4, no. 4, pp. 308-316, 2010

[11] Z. S. Zhang, Y. Z. Sun, J. Lin and G. J. Li, "Coordinated Frequency Regulation by Doubly Fed Induction Generator-Based Wind Power Plants," *IET Renewable Power Generation*, vol. 6, no. 1, pp. 38-47, 2012

[12] M. F. M. Arani and E. F. EI-Saadany, "Implementing Virtual Inertia in DFIG-Based Wind Power Generation," *IEEE Transactions on Power Systems*, vol. 28, no. 2, pp. 1373-1384, 2013

[13] K. V. Vidyanandan, N. Senroy, "Primary Frequency Regulation by Deloaded Wind Turbines Using Variable Droop," *IEEE Transactions on Power Systems*, vol. 28, no. 2, pp. 837-846, 2013

[14] A. Zertek, G. Verbic and M. Pantos, "A Novel Strategy for Variable-Speed Wind Turbines' Participation in Primary Frequency Control," *IEEE Transactions on Sustainable Energy*, vol. 3, no. 4, pp. 791-799, 2012

[15] F. Wilches-Bernal, J. H. Chow and J. J. Sanchez-Gasca, "A Fundamental Study of Applying Wind Turbines for Power System Frequency Control," *IEEE Transactions on Power Systems*, vol. 31, no. 2, pp. 1496-1505, 2016

[16] L. Wu and D. G. Infield, "Towards an Assessment of Power System Frequency Support From Wind Plant—Modeling Aggregate Inertial Response," *IEEE Transactions on Power Systems*, vol.28, no. 3, pp. 2283-2291, 2013

[17] J. Lee, E. Muljadi, P. Srensen and Y. C. Kang, "Releasable Kinetic Energy-Based Inertial Control of a DFIG Wind Power Plant," *IEEE Transactions on Sustainable Energy*, vol. 7, no. 1, pp. 279-288, 2016

[18] J. Lee, G. Jang, E. Muljadi, F. Blaabjerg, Z. Chen and Y. C. Kang, "Stable Short-Term Frequency Support Using Adaptive Gains for a DFIG-Based Wind Power Plant," *IEEE Transactions on Energy Conversion*, vol. 31, no. 3, pp. 1068-1079, 2016

[19] S. Kuenzel, L. P. Kunjumuhammed, B. C. Pal and I. Erlich, "Impact of Wakes on Wind Farm Inertial Response," *IEEE Transactions on Sustainable Energy*, vol. 5, no. 1, pp. 237-245, 2014

[20] V. Gevorgian, Y. Zhang and E. Ela, "Investigating the Impacts of Wind Generation Participation in Interconnection Frequency Response," *IEEE Transactions on Sustainable Energy*, vol. 6, no. 3, pp. 1004-1012, 2015

[21] Y. Liu, J. R. Gracia, T. J. King and Y. Liu, "Frequency Regulation and Oscillation Damping Contributions of Variable-Speed Wind Generators

in the U.S. Eastern Interconnection (EI)," *IEEE Transactions on Sustainable Energy*, vol. 6, no. 3, pp. 951-958, 2015

[22] M. Fischer, S. Engelken, N. Mihov and A. Mendonca, "Operational Experiences with Inertial Response Provided by Type 4 Wind Turbines," *IET Renewable Power Generation*, vol. 10, no. 1, pp. 17-24, 2016